How planar optical waves can be made to climb dielectric steps

MANFRED HAMMER,* ANDRE HILDEBRANDT, AND JENS FÖRSTNER

Theoretical Electrical Engineering, University of Paderborn, Warburger Straße 100, 33098 Paderborn, Germany
*Corresponding author: manfred.hammer@uni-paderborn.de

We show how to optically connect guiding layers at different elevations in a 3-D integrated photonic circuit. Transfer of optical power carried by planar, semi-guided waves is possible without reflections or radiation losses, and over large vertical distances. This functionality is realized through simple step-like folds of high-contrast dielectric slab waveguides, in combination with oblique wave incidence, and fulfilling a resonance condition. Radiation losses vanish, and polarization conversion is suppressed for TE wave incidence beyond certain critical angles. This can be understood by fundamental arguments resting on a version of Snell's law. The two 90° corners of a step act as identical partial reflectors in a Fabry–Perot-like resonator setup. By selecting the step height, i.e., the distance between the reflectors, one realizes resonant states with full transmission. Rigorous quasi-analytical simulations for typical silicon/silica parameters demonstrate the functioning. Combinations of several step junctions can lead to other types of optical on-chip connects, e.g., U-turn- or bridge-like configurations.   © 2015 Optical Society of America

The field of silicon photonics [1,2] holds promise for 3-D integration [3,4] with compact, high-contrast dielectric optical waveguides at different levels of photonic chips. This might concern small vertical distances, such that evanescent coupling between overlapping components becomes possible, but also concern optically well-separated waveguides at larger vertical separations. The latter scenario raises the question of how to transfer optical power between these distant layers. Conventional evanescent wave coupling [5] leads to either a device measured in centimeters, for vertical distances below a few hundreds of nanometers [5], or to a shorter device, but for a separation of not more than a few tens of nanometers [6]. More involved concepts for vertical coupling include waveguides with specifically tapered cores [7,8], radiative power transfer through grating couplers [9], and even resonant interaction through vertically stacked microrings [10].

Suppose that, given the task to connect guiding layers at different distant levels in the context of 3-D silicon photonics, and, being lured by the strong confinement properties of the high-contrast waveguides, one comes up with what might be perceived at first as a slightly "naive" approach of preparing a step-like structure as shown in Fig. 1(a), consisting of two sharp 90° corners with a vertical slab segment between them. As indicated in the schematic, the structure is assumed to be constant along the y axis, with half-infinite slabs parallel to the y–z plane. If operated in a standard 2-D setting with an incidence of vertically (x-) and laterally (y-) nonguided plane waves propagating in the positive z-direction normal to the interfaces, this structure clearly fails in view of the aforementioned task. Our simulation predicts a transmittance of merely $T = 3\%$ and a reflectance of $R = 11\%$. Most of the power is lost to radiation, and, thus, must be suspected as a potential source of unwanted crosstalk. Figure 1(b) shows the pronounced radiation losses.

Thus, it might come as a surprise to learn that the same step structure transfers *all* of the incident optical power to the upper level, if only the in-plane angle of incidence θ is set to 64°. A respective simulation predicts the profile of Fig. 1(c), with all fields nicely confined around the cores, and numerically perfect values of reflectance $R < 1\%$ and transmittance $T > 99\%$. It is the purpose of this Letter to highlight this effect and to provide a basic physical explanation. We refer to a more technical account [11] for details on the theoretical description and related studies. For all simulations in this Letter, we could rely on a rigorous, semi-analytical solver (vectorial quadridirectional eigenmode propagation, vQUEP) [12–14] for the vectorial 2-D problems. Figure 1 introduces parameters that are typical for a silicon photonics platform [15].

For a clarification of the full transmission effect, it is instrumental to look at a single corner first, as in Fig. 2(a). One notices that the structure is constant along the y axis. We assume that the slabs are single mode, supporting the fundamental guided TE_0 and TM_0 modes of both polarizations. For the parameters of Fig. 1, these are slab modes with effective mode indices $N_{TE0} = 2.823$ and $N_{TM0} = 2.040$.

The TE_0 mode is being sent toward the corner at angle θ. The incoming field thus exhibits an exponential dependence $\sim \exp(-ik_y y)$ with a given wavenumber $k_y = kN_{TE0} \sin \theta$
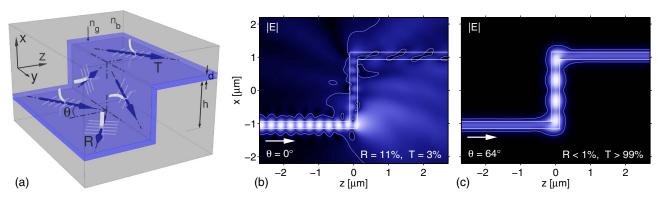
Fig. 1. Oblique incidence of semi-guided waves on a step configuration at angle θ: (a) schematic, (b) cross-section views of the optical electric field [absolute value $|\boldsymbol{E}|$, contour at 10% of the maximum field; the color bar of Fig. 2(e) applies] for normal incidence, and (c) at angle $\theta = 64°$. Parameters: refractive indices, $n_g = 3.45$ (slab cores) and $n_b = 1.45$ (cladding); slab thickness, $d = 220$ nm; vertical slab distance, $h = 1.868$ μm; incidence of TE polarized waves at vacuum wavelength, 1.55 μm.

for the vacuum wavenumber k. Aiming at a solution of the homogeneous Maxwell equations in the frequency domain, we may restrict the y-dependence of all fields to this single spatial Fourier component. Consequently, any outgoing mode, with an effective index N_{out} traveling at angle θ_{out} versus the x–z-plane, also shares this y-dependence. This can be stated in the form of Snell's law:

$$N_{out} \sin \theta_{out} = N_{TE0} \sin \theta. \qquad (1)$$

We look at outgoing TE_0 waves with $N_{out} = N_{TE0}$ first. For the reflected wave, Eq. (1) simply gives the law of reflection. The transmitted wave travels upward in the x–y-plane, guided by the vertical slab, at an angle θ. For outgoing TM_0 waves with $N_{out} = N_{TM0} < N_{TE0}$, one needs to distinguish between two cases. Equation (1) defines an angle θ_{out} only if $\sin \theta \, N_{TE0}/N_{TM0} \leq 1$, i.e., for small angles of incidence $\theta \leq \theta_m$ below a critical angle θ_m with $\sin \theta_m = N_{TM0}/N_{TE0}$, here $\theta_m = 46.27°$. Reflected and transmitted TM_0 waves then leave the corner region at angles θ_{out} given by Eq. (1).

For excitation at higher angles $\theta > \theta_m$, however, Eq. (1) does not apply. Any TM wave excited in the vicinity of the corner has to satisfy the local wave equation [16] with the externally enforced y-dependence. It does so by compensating for the too-large wavenumber k_y with an imaginary wavenumber in the direction of the outward axis ($-z$ for the reflected wave, x for the transmitted wave), i.e., the wave becomes evanescent, which concerns propagation in the x–z-plane. For $\theta > \theta_m$, one observes only outgoing TE waves "far away" from the corner.

Apart from the two guided modes, a continuum of nonguided modes with oscillatory behavior in the cladding region, and, with effective mode indices $N_{out} \leq n_b$ below the upper limit of the background refractive index n_b ("cladding modes"), can be associated with the horizontal and vertical slabs. Applying the former arguments to the modes of this radiation continuum, one finds that all of these modes become x–z-evanescent, if $\sin \theta \, N_{TE0}/n_b \geq 1$. Consequently, all radiation losses vanish for $\theta > \theta_b$ with $\sin \theta_b = n_b/N_{TE0}$, here $\theta_b = 30.91°$. Note that the reasoning for the critical angles (see [11] for a more formal and general account) depends on the properties of the outgoing slab waveguides only, irrespective of, e.g., the corner shape (rounding) or the corner angle.

Similar arguments apply for plane-wave scattering from cylinders at oblique incidence [17,18], for slab waveguides with straight discontinuities, typically end facets, with oblique incidence of guided modes [16,19–21], and for slab waveguides with periodic corrugations at oblique incidence [22,23]. So far, however, we have not encountered this reasoning in the case of noncoplanar slabs. When adapted to the present configurations, the frequency-domain Maxwell equations coincide formally with the equations that govern the modes of 3-D channel waveguides, where the present wavenumber k_y takes the role of the propagation constant; the problems differ with respect to boundary conditions [16]. The suppression of radiation losses can then be understood in terms of an angle-dependent, negative effective permittivity [11,16]. The same effect enables the formation of guided modes in channel waveguides with 2-D confinement.

Figure 2(b) shows the power transmission properties of the corner structure relating to the fundamental guided modes, as a function of the angle of incidence. The critical angles θ_b and θ_m are indicated. At normal incidence $\theta = 0$, the otherwise vectorial equations split into the standard scalar 2-D Helmholtz problems for TE and TM waves; thus, there is no polarization conversion. The moderate transmittance and reflectance levels of $T_{TE} = 14\%$, $R_{TE} = 13\%$, and $T_{TM} = R_{TM} = 0$ relate to pronounced radiation losses, clearly evident in the field profile in Fig. 2(c).

Radiation losses, and, thus, all fields outside the evanescent tails around the slab cores, vanish for wave incidence at angles beyond θ_b. Strong polarization conversion is observed, with an extreme value of TM transmission at $\theta = 36.5°$, with transmittance and reflectance levels of $T_{TE} = 10\%$, $R_{TE} = 26\%$, $T_{TM} = 63\%$, and $R_{TM} = 1\%$. The reflected guided waves of both polarizations lead to a slightly irregular beating pattern of the partly standing, partly traveling waves in the horizontal slab [see Fig. 2(d)]. In the vertical slab, the strong TM contribution manifests in the large electric fields immediately outside the core. (The absolute value $|\boldsymbol{E}|$ of the electric field vector is shown.) Upward traveling TE and TM waves, with unequal amplitudes, cause a weak beating pattern, barely visible in the figure.

The polarization conversion is suppressed at even higher angles of incidence for $\theta > \theta_m$. The field profile in panel (e)
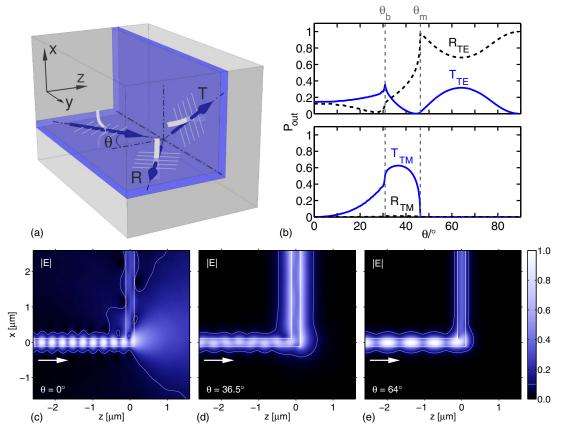
Fig. 2. Linear 90° waveguide corner at oblique incidence: (a) schematic, (b) modal reflectances R_{TE} and R_{TM} and transmittances T_{TE} and T_{TM} versus the angle of incidence θ (TE$_0$ and TM$_0$ modes); and field profiles (absolute value $|\boldsymbol{E}|$ of the electric field, contour at 10% of the field maximum) for angles of incidence (c) $\theta = 0°$, (d) $\theta = 36.5°$, and (e) $\theta = 64°$. See the caption for Fig. 1 for parameters.

of Fig. 2, for incidence at $\theta = 64°$ with extreme levels $T_{TE} = 32\%$, $R_{TE} = 68\%$, and $T_{TM} = R_{TM} = 0$, shows a tight field confinement around the slab cores. Note that this is still a vectorial problem in which TM waves play a role in the solution; their contribution, however, remains restricted to the immediate vicinity of the corner (here at the origin), because of their x–z-evanescent behavior.

Having clarified some properties of the constituting corners, we now resume the discussion of the step structure. With a view to the aim of large power transfer, we select the angle of incidence $\theta = 64°$ that leads to the TE transmission maximum of the separate corners. All former arguments on suppression of radiation losses, and on suppression of polarization conversion, rely on the properties of the outgoing slabs only, without any reference to the particular shape of the structure that connects these outlets. Thus, we can expect that, at this angle of incidence and for identical slab properties, neither radiation losses nor conversion to TM occur when the step is being excited by the TE$_0$ wave.

Further, we assume that the intermediate vertical segment is of sufficient height h, such that any x–z-evanescent fields (of either TE or TM polarization) that are being excited at one of the corner points, are negligible in the region around the other respective corner. Then only the upward and downward traveling TE$_0$ waves remain that mediate between the corners. These waves and the incoming, reflected, and transmitted

TE$_0$ waves in the horizontal slabs propagate at the same angle θ with respect to the x–z-plane. They share the uniform harmonic y-dependence, which can then be disregarded for the discussion of the propagation along the slab cores.

Consequently, we may view the step as a system of two identical partial reflectors, the corners, with counterpropagating waves of a single polarization in between, i.e., as a system akin to a Fabry–Perot-interferometer [24]. Here, the step height h plays the role of the distance between the two reflectors. Accordingly, the scan over h in Fig. 3 reveals a regular series of resonances. One of the extreme states with full transmission has been selected for the example in Fig. 1(c).

For a sufficiently large h, e.g., $h > 0.75$ μm, the maxima in T_{TE} with unit transmittance appear regularly at distances of $\Delta h = \lambda/(2N_{TE0} \cos\theta) = 626$ nm. Here, $kN_{TE0} \cos\theta$ is the wavenumber component relevant for the propagation in the $\pm x$ direction. Originating from a resonance effect, these states depend more or less critically on all parameters that enter. Concerning the step height h, in Fig. 3 one observes levels $T_{TE} > 99\%|90\%|75\%|50\%$ for intervals of full width $\Delta h = 8$ nm$|25$ nm$|44$ nm$|77$ nm around the peak centers. Considering the operation wavelength as a further example, respective simulations show transmittance levels $T_{TE} > 99\%|90\%|75\%|50\%$ for spectral intervals of widths $\Delta \lambda = 4$ nm$|13$ nm$|23$ nm$|40$ nm, centered on the design wavelength $\lambda = 1.55$ μm. The 50% transmittance window thus covers
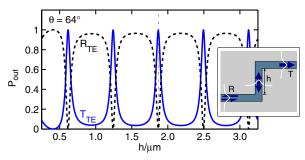
Fig. 3. For the step configuration of Fig. 1(a): transmittance T_{TE} and reflectance R_{TE} as a function of the step height h. The indicated level $h = 1.868$ µm relates to Figs. 1(b) and 1(c).

the entire C-band of infrared optical communications. Note that radiation losses and polarization conversion are suppressed fully within the given intervals; the nontransmitted part of the incident power is reflected as a semi-guided TE_0 wave.

Beyond the selection of a corner configuration with high transmission and the height scan in Fig. 3, no particular optimization has been necessary to identify step configurations with good performance. Within certain limits, this procedure can be reversed into an approach of fixing a step height first, followed by an angular scan. Nevertheless, there is plenty of room left for further optimization, aiming, e.g., at lossless corner configurations with higher transmittance. This should lead to steps with less critical resonance conditions, i.e., with improved spectral tolerances and generally relaxed tolerance requirements. Further studies could also investigate the incidence of TM waves, and, thus, the configurations in which both propagating TE and TM waves connect the corners. While, so far, these are
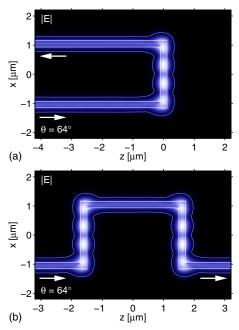
evidently quasi-3-D concepts at best, the effect can be transferred to "real" 3-D by considering oblique incidence of laterally wide semi-guided beams with narrow angular spectrum [11].

In conclusion, we have shown that semi-guided planar optical waves *can* be made to climb steps without radiation losses, polarization conversion, or reflections. This is achieved for simple dielectric slabs with relatively modest means of oblique incidence, combined with a Fabry–Perot-like resonance effect. One might compare this with concepts relying on line defects in photonic crystals, various types of (lossy) plasmonic wave confinement, and specific corner geometries [25] in conventional high-contrast dielectric waveguides.

Extension to other, perhaps more intriguing, examples is obvious. For sufficient step height, one of the corners in a step can be mirrored without affecting the transmission. Steps can be concatenated with intermediate slab segments of arbitrary length. Our simulations predict modal transmittance values $T_{TE} > 99\%$ for both structures in Fig. 4.

REFERENCES

1. R. Soref, IEEE J. Sel. Top. Quantum Electron. **12**, 1678 (2006).
2. P. Koonath, T. Indukuri, and B. Jalali, J. Lightwave Technol. **24**, 1796 (2006).
3. P. Prakash Koonath and B. Jalali, Opt. Express **15**, 12686 (2007).
4. N. Sherwood-Droz and M. Lipson, Opt. Express **19**, 17758 (2011).
5. R. A. Soref, E. Cortesi, F. Namavar, and L. Friedman, IEEE Photon. Technol. Lett. **3**, 22 (1991).
6. J. K. Doylend, A. P. Knights, C. Brooks, and P. E. Jessop, Proc. SPIE **5970**, 59700G (2005).
7. R. Sun, M. Beals, A. Pomerene, J. Cheng, C.-Y. Hong, L. Kimerling, and J. Michel, Opt. Express **16**, 11682 (2008).
8. J. F. Bauters, M. L. Davenport, M. J. R. Heck, J. K. Doylend, A. Chen, A. W. Fang, and J. E. Bowers, Opt. Express **21**, 544 (2013).
9. P. Dong and A. G. Kirk, Proc. SPIE **5357**, 135 (2004).
10. J. T. Bessette and D. Ahn, Opt. Express **21**, 13580 (2013).
11. M. Hammer, A. Hildebrandt, and J. Förstner, "Full resonant transmission of semi-guided planar waves through slab waveguide steps at oblique incidence," arXiv:1502.07619 (2015).
12. M. Hammer, Opt. Commun. **338**, 447 (2015).
13. M. Hammer, Opt. Commun. **235**, 285 (2004).
14. M. Hammer, "METRIC—mode expansion tools for 2D rectangular integrated optical circuits," http://metric.computational-photonics.eu/.
15. W. Bogaerts, R. Baets, P. Dumon, V. Wiaux, S. Beckx, D. Taillaert, B. Luyssaert, J. Van Campenhout, P. Bienstman, and D. Van Thourhout, J. Lightwave Technol. **23**, 401 (2005).
16. F. Çivitci, M. Hammer, and H. J. W. M. Hoekstra, Opt. Quantum Electron. **46**, 477 (2014).
17. J. R. Wait, Can. J. Phys. **33**, 189 (1955).
18. H. Wang and G. Nakamura, Appl. Numer. Math. **62**, 860 (2012).
19. S.-T. Peng and A. Oliner, IEEE Trans. Microwave Theory Tech. **29**, 843 (1981).
20. T. P. Shen, R. F. Wallis, A. A. Maradudin, and G. I. Stegeman, J. Opt. Soc. Am. A **4**, 2120 (1987).
21. W. Biehlig and U. Langbein, Opt. Quantum Electron. **22**, 319 (1990).
22. K. Wagatsuma, H. Sakaki, and S. Saito, IEEE J. Quantum Electron. **15**, 632 (1979).
23. J. Van Roey and P. E. Lagasse, Appl. Opt. **20**, 423 (1981).
24. M. Born and E. Wolf, *Principles of Optics*, 7th ed. (Cambridge University, 1999).
25. R. U. Ahmad, F. Pizzuto, G. S. Camarda, R. L. Espinola, H. Rao, and R. M. Osgood, IEEE Photon. Technol. Lett. **14**, 65 (2002).

Fig. 4. (a) U-turn and (b) bridge configurations with full transmission of semi-guided TE waves at oblique incidence; absolute value $|E|$ of the optical electric field, contour at 10% of the maximum level; see the color bar of Fig. 2(e). Parameters are as in Fig. 1(c), with a 3 µm slab segment as the upper level of the bridge (b).